CrossMark

Magnetoresistance of nanocomposite copper/carbon thin films

Ali Arman[1] · Carlos Luna[2] · Mohsen Mardani[1] · Fatemeh Hafezi[1] ·
Amine Achour[3] · Azin Ahmadpourian[4]

Abstract Nanocomposite thin films made of partially oxidized Cu nanoparticles embedded into hydrogenated amorphous carbon, with different thicknesses and Cu/C ratio, were prepared by means of radio frequency plasma enhanced chemical vapor deposition and radio frequency sputtering using acetylene gas and copper target. The surface roughness was investigated using atomic force microscopy, revealing the fractal geometry of the Cu/carbon thin films at the nanoscale with fractal dimensions around 2.7. In addition, the electrical properties of these films and their dependence on the application of low magnetic fields were explored at room temperature. It was found that when the Cu nanoparticles are separated by gaps, the electrical conduction is governed by tunneling effects. In these conditions, the samples exhibit negative magnetoresistance values, displaying steps in the dependences on the magnetic field. These properties suggest the potential use of these films as magnetic sensors in spintronics.

✉ Ali Arman
ali.arman173@gmail.com

✉ Azin Ahmadpourian
Azinahmadpourian@gmail.com

1 Vacuum Technology Group, ACECR Sharif Branch, Tehran, Iran

2 Universidad Autónoma de Nuevo León, Av. Universidad s/n, 66455 San Nicolás de los Garza, Nuevo León, Mexico

3 Institut National de la Recherche Scientifique (INRS), 1650 Boulevard Lionel-Boulet, Varennes, QC J3X 1P7, Canada

4 Department of Physics, Kermanshah Branch, Islamic Azad University, Kermanshah, Iran

1 Introduction

Metallic thin films and nanostructures have attracted huge attention due to their new electrical conductivity phenomena. For instance, in Cu thin films, evidences of electron quantum localization in 2D metallic materials such as negative magnetoresistance (i.e., the electrical resistance decreases in presence of a magnetic field) and an anomalous logarithmic increase of the electrical resistance in small perpendicular fields at low temperatures have been theoretically predicted [1–4], and experimentally proved [5, 6]. On the other hand, thin films present obvious technological potential for prospective electronic devices based on the 2D electronic transport and the polarization of the electron spin [6–10]. However, the negative magnetoresistance phenomenon is rarely observed at room temperature [5, 6].

The physical and physicochemical properties of thin films strongly depend on the composition, thickness, surface roughness, structure and the presence of impurities and crystalline defects, which in turn, depend on the preparation method of samples and the synthetic conditions. In this regard, the sputtering method [11] and the chemical vapor deposition techniques [12] are especially versatile routes for the preparation of nanostructured and/or multilayer thin films, whose combination can yield to the preparation of thin nanocomposite films with engineered electrical resistance through the mixture of conductive and dielectric materials [13–15].

The development of more accurate methodologies for the characterization of thin films is an essential subject for understanding the interesting physical phenomena that exhibit these advanced materials. With this aim in mind, several works have recently carried out fractal analysis of the atomic force microscopy (AFM) measurements to

Table 1 Compositions, thickness and preparation conditions of the three thin nanocomposite films

ID	RF sputtering			
	Thickness (nm)	Deposition Time (min)	RF power (W)	Initial acetylene gas pressure (mbar)
#1	113	20	180	0.035
#2	100	20	200	0.045
#3	60	20	180	0.040
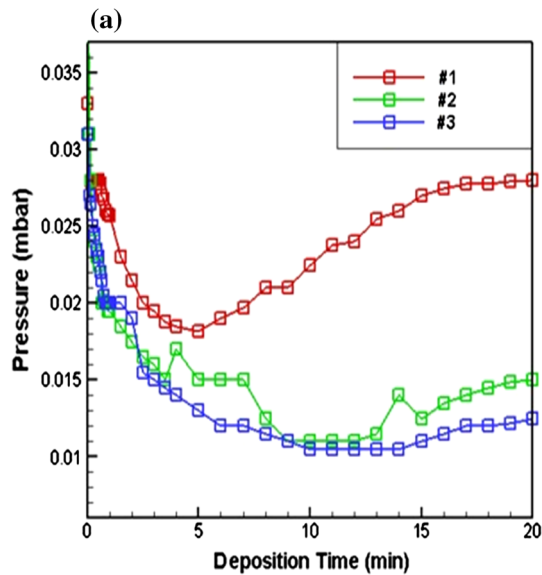
Fig. 1 Pressure of the sample chamber as a function of the deposition time for samples 1, 2 and 3

precisely characterize the 3D surface roughness of thin films [16–20].

In the present work, nanocomposite thin films composed by partially oxidized Cu nanoparticles embedded into hydrogenated amorphous carbon matrix were prepared by means of a combination of RF-plasma enhanced chemical vapor deposition and RF-sputtering using acetylene gas and copper target at room temperature. The RF power and the initial acetylene gas pressure were varied in order to obtain thin films with different thicknesses and Cu/C ratio for comparison purpose. The surface roughness of these low dimensional materials was investigated by atomic force microscopy and fractal analyzes, while the electrical conductivity of the samples was investigated in the presence of magnetic fields. Herein, the negative magnetoresistance phenomenon was observed at room temperature. These results show that these nano-composites are promising for magnetic sensors and spintronics applications.
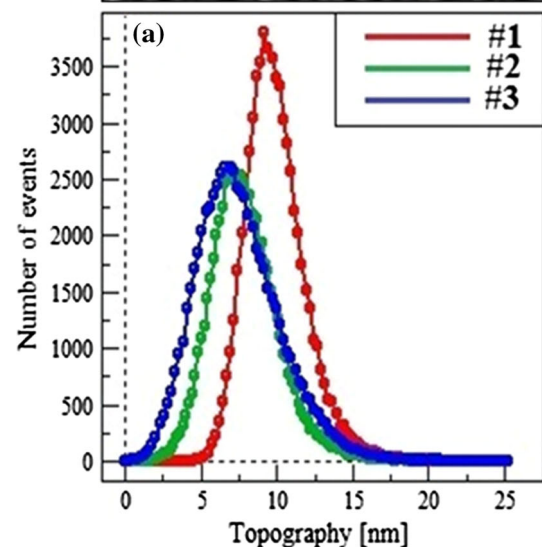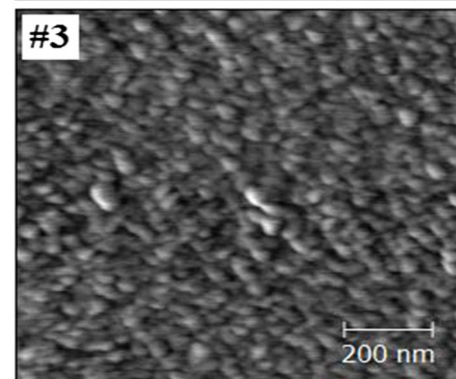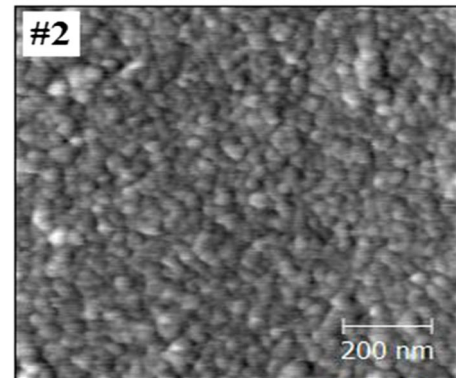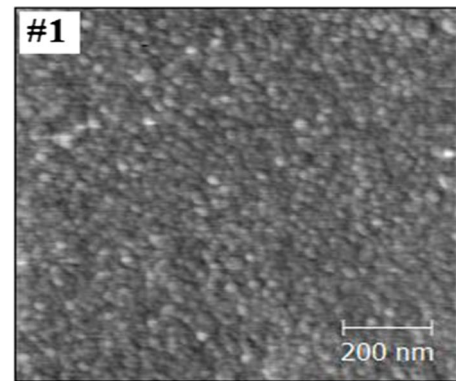
◄**Fig. 2** Representative AFM images of samples 1, 2 and 3, respectively, for scanning areas of 1.0 μm × 1.0 μm. **a** Particle size distributions (height distributions) of samples 1, 2 and 3, respectively

2 Experimental details

2.1 Preparation of samples

A radio frequency plasma enhanced chemical vapor deposition (RF-PECVD) set-up was employed to produce Cu nanoparticles embedded into hydrogenated amorphous carbon matrix with different thicknesses and Cu/C ratio. In this configuration, the acetylene gas was used as reactant and bombardment gas. In consequence, sputtered target materials and products of the reactant gas formed the resulting thin films. Two rotary and diffusion pumps were used to reach the required vacuum in the steel chamber. The chamber contained two electrodes with different surface areas. The smaller electrode (7.5 cm in diameter), with a copper target, was connected to the RF source, while the other electrode (13 cm in diameter) was grounded through the body of the stainless steel chamber. The electrodes were positioned at a separation distance of 5 cm. The deposition was carried out on glass and silicon substrates on the grounded electrode at room temperature using a RF frequency of 13.56 MHz and power of 200 or 180 W. The initial gas pressure was set at different pressures (0.035, 0.040 and 0.045 mbar) in order to observe any change in the properties of the resulting films. The final samples were named 1, 2 and 3, respectively. The synthesis conditions and some characteristics of these samples are summarized in Table 1.

2.2 Characterization techniques

The surface morphology properties of the three samples were studied by AFM using a Nanoscope Multimode atomic force microscope (Digital Instruments, Santa Barbara, CA) in non-contact mode, determining the average nanoparticles size and the Root Mean Square (RMS) roughness. The 3D complexity of the thin films was investigated through fractal analysis applied to the original AFM files using the cube counting method (derived directly from a definition of box-counting fractal dimension) with a linear interpolation type [Mountains Map \circledR 7 Software (Digital Surf, Besançon, France)]. In this analysis, the fractal dimension, D_f, was estimated, which has a value within the range $2 \leq D_f \leq 3$ [21–23].
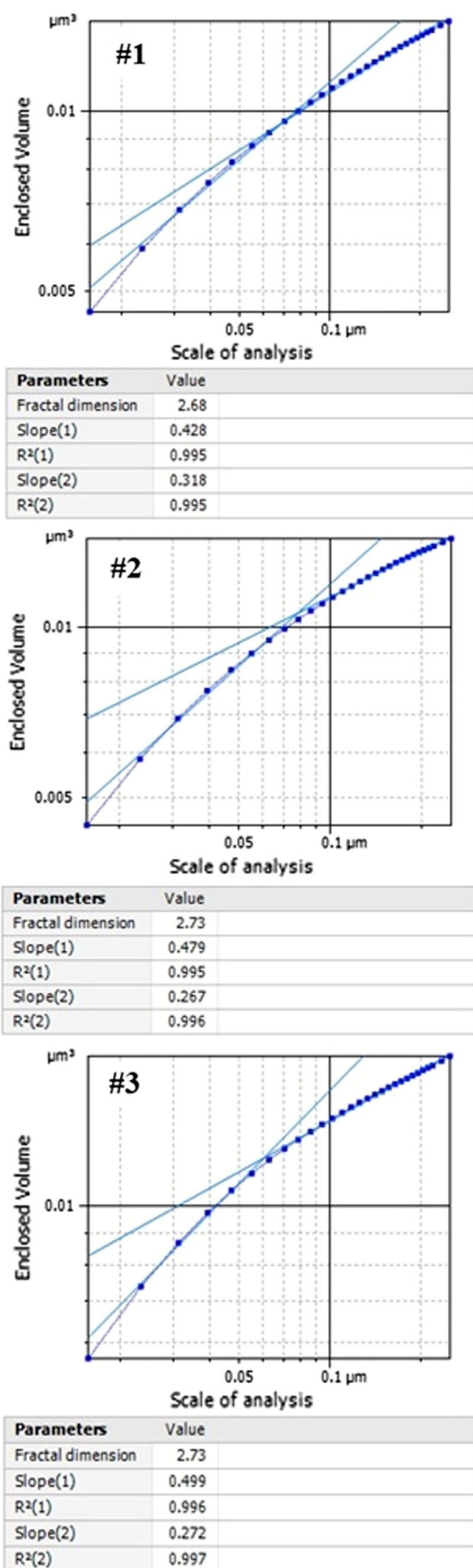
The magnetoresistance, which is defined as the percentage ratio $100 \times [R(H) - R(0)]/R(0)$ being R the electrical resistance, was measured at room temperature with a variable magnetic field applied parallel to the film plane for the three samples.

3 Results and discussion

The growth mechanism of the copper samples was investigated by analyzing the dependence of the pressure in the sample chamber on the deposition time (Fig. 1). For the three samples studied in the present contribution, it was observed that the pressure initially decreases (until the fifth minute of deposition for sample 1, and until the thirteenth minute for samples 2 and 3).According to previous studies [23–25], the decreasing of the initial pressure during the first minutes can be related to the high deposition rate of hydrocarbon ions forming a carbon layer onto the substrate. In such case, the pressure decreases because the rate of deposition of carbon is higher than the rate of incoming hydrocarbon gas to the chamber. Also, a small reactive sputtering of copper could occur. When the pressure reaches values around 0.02 mbar, the ions generated from acetylene have enough energy for sputtering the Cu target, therefore, with the presence of sputtered Cu and the hydrocarbon ions, the pressure inside the chamber

Table 2 Basic properties of the height values distribution (including its variance, skewness and kurtosis) of the surface samples for scanning square areas of 1.0 μm × 1.0 μm

The statistical parameters	Symbol	Sample (#1) Values	Sample (#2) Values	Sample (#3) Values
Height parameters				
Root mean square height	Sq (nm)	1.97	2.21	2.80
Skewness	Ssk (-)	0.803	0.603	0.725
Kurtosis	Sku (-)	4.60	3.97	4.17
Maximum peak height	Sp (nm)	14.8	12.1	17.8
Maximum pit height	Sv (nm)	10	7.99	7.63
Maximum height	Sz (nm)	24.8	20.1	25.5
Arithmetic mean height	Sa (nm)	1.52	1.72	2.19
Inclination θ (°)	–	0.2	0.2	0.2
Inclination φ (°)	–	23	15	52.3

#1 Parameters	Value
Fractal dimension	2.68
Slope(1)	0.428
R²(1)	0.995
Slope(2)	0.318
R²(2)	0.995

#2 Parameters	Value
Fractal dimension	2.73
Slope(1)	0.479
R²(1)	0.995
Slope(2)	0.267
R²(2)	0.996

| #3 Parameters	Value
Fractal dimension	2.73
Slope(1)	0.499
R²(1)	0.996
Slope(2)	0.272
R²(2)	0.997

◄**Fig. 3** Enclosed volume for the three samples as a function of the scale of analysis

increases. The increase of pressure should continue until the mean ion energy gets reduced again below the threshold energy needed for sputtering. This point is the cutoff of physical sputtering of copper target [23]. According to these considerations, one can deduce from the curves of Fig. 1 that the copper content of sample 1 is the highest in comparison with the other samples, while the copper content in sample 2 is higher than that in sample 3. In other words, the sample 1 should have the lowest carbon content, while carbon concentration should increase for sample 2 and 3, respectively.

AFM analysis and topography curves are shown in Fig. 2. As can be seen in this figure, the average size of nanoparticles is around 6 nm for sample 1 and sample 2, and 10 nm for sample 3 (see the particle height distribution obtained from AFM characterization in Fig. 2a). The analysis of these images (with the Digital Surf Mountains Map® Premium software version 7.0) gave roughness values of 1.97, 2.21 and 2.80 for samples 1, 2 and 3, respectively. Table 2 depicts the basic properties of the height values distribution of the surface samples (including its variance, skew and kurtosis). In addition, to gain more information about the characteristics of the film surface, the AFM data were analyzed using the cube counting method. Figure 3 shows the dependence of the calculated volume for surfaces on the scale of analyses (size of the structuring elements) associated with the AFM images. The fractal dimension was calculated from the slope of the best fits of regression lines (shown in Fig. 3) [26, 27]. It is observed that the fractal dimension was rather similar for the three samples (2.68, 2.73 and 2.73 for samples 1, 2, and 3, respectively).

The electrical resistance of samples was measured as a function of the applied magnetic field (Fig. 4). The obtained results show values of the electrical resistance for samples 3 and 2 around 1700 and 5 MΩ, respectively, while the electrical resistance was about 3.3 Ω for sample 1. This dramatic difference in the electrical resistance properties is due to differences in the sputtered copper content in the samples; the electrical conductivity increases as the copper content is increased and the aggregation of the Cu nanoparticles is improved. On the other hand, for samples 2 and 3, the electrical resistance at room temperature decreased with increasing external magnetic field, leading to negative magnetoresistance (MR) values. Such behavior is usually observed at low temperatures [5, 6]. This behavior is probably due to the decrease of the spin disorder with the presence of the exciting magnetic field. In order to explain the magnetoresistance properties of the studied nanostructured copper/carbon thin films, three
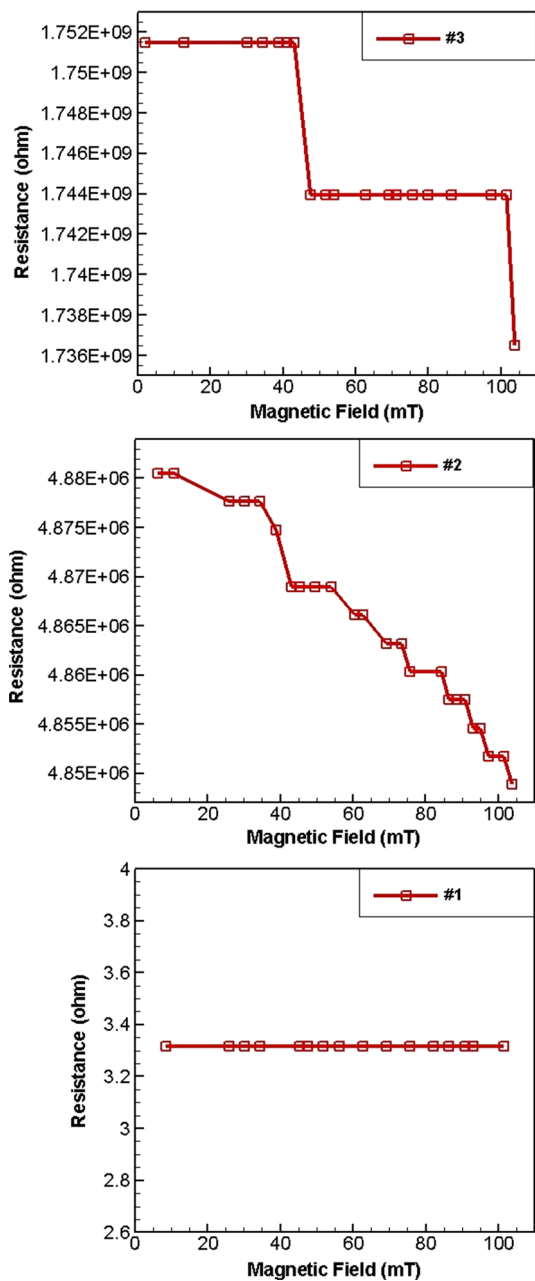
Fig. 4 Low field MR of the three prepared and studied nanostructured copper/carbon thin films

regions or stages of the samples can be distinguished in agreement with their electrical behavior as follows: (i) dielectric stage, in which the particles are separated by gaps, (ii) transition stage, in which the aggregation of nanoparticles starts to occur, and (iii) metallic stage, in which the nanoparticles are in contact and they are not arranged as isolated nanoparticles. Thus, the electrical resistance in composite systems with insulator and conductive phases is related to two different mechanisms: tunneling between conductive particles that are separated by insulator layers, and percolation in a continuous metallic network of

particles. The insets of Fig. 2 show 2D AFM images of the samples with high contrast of the sample, where the darkest regions are related to empty areas of particles. It is obvious that in sample 3 the nanoparticles are situated in separated islands. Hence, adjacent particles are not in direct contact and nanometric distances separate them. Therefore, the electron transport between neighboring nanoparticles should occur by tunneling effect. However, more particles are aggregated as the copper particles content is increased reaching the transition region (stage ii) and metallic channels are created at the surface. This is probably the case of sample 2. In this situation, the conduction occurs through percolation between metallic clusters composed from copper nanoparticles. Interestingly, the variation of the MR with the magnetic field displays a step behavior that we tentatively ascribe to the presence of copper oxide phases (that behave as semiconductor) on the nanoparticles surface of samples 2 and 3, in agreement with Rutherford Backscattering measurements (data not shown). In sample 1, the magnetoresistance effects were not observed because the Cu nanoparticles are in contact and the sample is in a metallic stage.

4 Conclusion

Thin nanocomposite films constituted by partially oxidized Cu nanoparticles embedded into hydrogenated amorphous carbon matrix have been obtained using a combination of RF-PECVD coupled with a RF-sputtering method. The thickness and the Cu/C atomic content ratio were modulated with the variation of the RF power and the initial gas pressure. The average size of nanoparticles for the three studied samples was around 6 or 10 nm. The reduction of the thickness from 113 to 60 nm yielded to the increment of the roughness of the films from 1.97 to 2.8, whereas the fractal dimension for the three samples was around 2.7. In addition, the electrical resistance increased from 3.3 Ω to 1700 MΩ at room temperature as the nanoparticles were separated between them by nanometric gaps and the electrical conduction occurred by a tunneling phenomenon. In these conditions, the samples exhibited negative magnetoresistance values, displaying steps in the dependences on the magnetic field.

References

1. D.C. Licciardello, D.J. Thouless, Conductivity and mobility edges for two-dimensional disordered systems. J. Phys. C: Solid. State Phys. **8**(24), 4157–4170 (1975)
2. D.J. Thouless, Maximum metallic resistance in thin wires. Phys. Rev. Lett. **39**(18), 1167 (1977)

3. D.C. Licciardello, D.J. Thouless, Conductivity and mobility edges in disordered systems. II. Further calculations for the square and diamond lattices. J. Phys. C: Solid State Phys. **11**(5), 925–936 (1978)

4. E. Abrahams, P.W. Anderson, D.C. Liciardello, T.V. Ramakrishnan, Scaling theory of localization: absence of quantum diffusion in two dimensions. Phys. Rev. Lett. **42**(10), 673–676 (1979)

5. C. Van Haesendonck, L. Van den dries, Y. Bruynseraede, G. Deutscher, Localization and negative magnetoresistance in thin copper films. Phys. Rev. B. **25**(8), 5090–5096 (1982)

6. D. Abraham, R. Rosenbaum, Magnetoresistance of thin copper films. Phys. Rev. B. **27**(2), 1413–1416 (1983)

7. D. Pesin, A.H. MacDonald, Spintronics and pseudospintronics in graphene and topological insulators. Nat. Mater. **11**, 409–416 (2012)

8. M. Vazquez, C. Luna, M.P. Morales, R. Sanz, C.J. Serna, C. Mijangos, Magnetic nanoparticles: synthesis, ordering and properties. Phys. B: Condens. Matter **354**(1), 71–79 (2004)

9. C. Luna, M. Ilyn, V. Vega, V.M. Prida, J. González, R. Mendoza-Reséndez, Size distribution and frustrated antiferromagnetic coupling effects on the magnetic behavior of ultrafine akaganéite (ß-FeOOH) nanoparticles. J. Phys. Chem. C **118**(36), 21128–21139 (2014)

10. S. Naderi, M. Shahrokhi, H.R. Noruzi, A. Gurabi, R. Moradian, Structural, electronic and magnetic properties of Fe and Co monatomic nanochains encapsulated in BN nanotube bundle. Eur. Phys. J. Appl. Phys. **62**(03), 30402 (2013)

11. T. Ghodselahi, A. Arman, Magnetoresistance of Cu–Ni nanoparticles in hydrogenated amorphous carbon thin films. J. Mater. Sci.: Mater. Electron. **26**(6), 4193–4197 (2015)

12. N. Ghobadi, M. Ganji, C. Luna, A. Arman, A. Ahmadpourian, Effects of substrate temperature on the properties of sputtered TiN thin films. J. Mater. Sci.: Mater. Electron. **27**(3), 2800–2808 (2016)

13. J. Kong, A.M. Cassell, H. Dai, Chemical vapor deposition of methane for single-walled carbon nanotubes. Chem. Phys. Lett. **292**(4), 567–574 (1998)

14. M. Molamohammadi, A. Arman, A. Achour, B. Astinchap, A. Ahmadpourian, A. Boochani, S. Naderi, A. Ahmadpourian, Microstructure and optical properties of cobalt–carbon nanocomposites prepared by RF-sputtering. J. Mater. Sci.: Mater. Electron. **26**(8), 5964–5969 (2015)

15. T. Ghodselahi, M.A. Vesaghi, A. Gelali, H. Zahrabi, S. Solaymani, Morphology, optical and electrical properties of Cu–Ni nanoparticles in aC:H prepared by co-deposition of RF-sputtering and RF-PECVD. Appl. Surf. Sci. **258**(2), 727–731 (2011)

16. T. Ghodselahi, M.A. Vesaghi, A. Shafiekhani, M. Ahmadi, M. Panahandeh, M. HeidariSaani, Metal–nonmetal transition in the copper–carbon nanocomposite films. Phys. B: Condens. Matter **405**(18), 3949–3951 (2010)

17. A. Arman, T. Ghodselahi, M. Molamohammadi, S. Solaymani, H. Zahrabi, A. Ahmadpourian, Microstructure and optical properties of Cu@Ni nanoparticles embedded in aC:H. Prot. Met. Phys. Chem. Surf. **51**(4), 575–578 (2015)

18. S. Talu, S. Stach, V. Sueiras, N.M. Ziebarth, Fractal analysis of AFM images of the surface of Bowman's membrane of the human cornea. Ann. Biomed. Eng. **43**(4), 906–916 (2015)

19. S. Talu, S. Stach, T. Lainovic, M. Vilotic, L. Blazic, S.F. Alb, D. Kakas, Surface roughness and morphology of dental nanocomposites polished by four different procedures evaluated by a multifractal approach. Appl. Surf. Sci. **330**, 20–29 (2015)

20. S. Talu, A.J. Ghazai, S. Stach, A. Hassan, Z. Hassan, M. Talu, Characterization of surface roughness of Pt Schottky contacts on quaternary n-Al0. 08In0. 08Ga0. 84N thin film assessed by atomic force microscopy and fractal analysis. J. Mater. Sci.: Mater. Electron. **25**(1), 466–477 (2014)

21. A. Gelali, A. Ahmadpourian, R. Bavadi, M.R. Hantehzadeh, A. Ahmadpourian, Characterization of microroughness parameters in titanium nitride thin films grown by DC magnetron sputtering. J. Fusion Energy **31**(6), 586–590 (2012)

22. S. Stach, D. Dallaeva, S. Talu, P. Kaspar, P. Tomanek, S. Giovanzana, L. Grmela, Morphological features in aluminum nitride epilayers prepared by magnetron sputtering. Mater. Sci.-Pol. **33**(1), 175–184 (2015)

23. A. Arman, Ş. Ţălu, C. Luna, A. Ahmadpourian, M. Naseri, M. Molamohammadi, Micromorphology characterization of copper thin films by AFM and fractal analysis. J. Mater. Sci.: Mater. Electron. **26**(12), 9630–9639 (2015)

24. S. Kulesza, M. Bramowicz, A comparative study of correlation methods for determination of fractal parameters in surface characterization. Appl. Surf. Sci. **293**, 196–201 (2014)

25. T. Ghodselahi, M.A. Vesaghi, A. Shafiekhani, A. Baradaran, A. Karimi, Z. Mobini, Co-deposition process of RF-sputtering and RF-PECVD of copper/carbon nanocomposite films. Surf. Coat. Technol. **202**(12), 2731–2736 (2008)

26. M. Molamohammadi, C. Luna, A. Arman, S. Solaymani, A. Boochani, A. Ahmadpourian, A. Shafiekhani, Preparation and magnetoresistance behavior of nickel nanoparticles embedded in hydrogenated carbon film. J. Mater. Sci.: Mater. Electron. **26**(9), 6814–6818 (2015)

27. D. Dallaeva, S. Talu, S. Stach, P. Skarvada, P. Tomanek, L. Grmela, AFM imaging and fractal analysis of surface roughness of AlN epilayers on sapphire substrates. Appl. Surf. Sci. **312**, 81–86 (2014)